Towards Power Optimized Kalman Filter for Gait Assessment using Wearable Sensors

Prem Santosh Udaya Shankar, Nikhil Raveendranathan, Nicholas R. Gans and Roozbeh Jafari
University of Texas at Dallas
Department of Electrical Engineering
{pxu080020, nxr072100, ngans, rjafari}@utdallas.edu

ABSTRACT

Systems with wearable and wireless motion sensors have been receiving significant attention in the past few years specifically for the applications of human movement monitoring. One important concern in the design of wearable and wireless motion sensors, also referred to as Body Sensor Networks, is the form factor. A smaller form factor makes the device easily portable and wearable, hence improving users' acceptability. The form factor is usually determined by the size of the battery, which in turn is dependent on the power required by the system and the sensors present in it. Most human movement monitoring applications require inertial sensors like accelerometers and gyroscopes. However, the power consumption of a gyroscope is an order of magnitude greater than an accelerometer. In this paper, we examine power savings obtained by turning off the gyroscope for short periods while using Kalman filters to predict the state. The Kalman filter uses previous readings from both accelerometer and gyroscopes for its calculations. Our results show that with this approach, the system can achieve a reasonable reduction in power consumption with an acceptable loss of accuracy.

Keywords

Body Sensor Networks, Displacement Estimation, Kalman Filter, Power Optimization

1. INTRODUCTION

Wireless sensing technologies and embedded computing have advanced rapidly over the last decade. This motivated researchers to look into various applications that were previously unattainable. Body Sensor Networks (BSNs), being a subset of wireless sensor networks, use certain wearable sensor nodes to track motion and other significant signals from the human body. The system, being inexpensive and easily wearable, enables applications in the health care domain [17]. Some other domains using BSNs are sport training [10] and gait analysis [4]. The system could also be incorporated into telemedicine, resulting in the support of early detection and prevention of certain abnormalities.

Gait analysis, which is the assessment of human movements during walking, is one of the most important applications of BSN. It has been widely used for fall detection [8], physical rehabilitation[12] and in assessment of diseases which involve gait disorders like Parkinson's disease[16, 19]. The motor movements are generally monitored with inertial motion sensors such as accelerometers and gyroscopes. These sensing devices are called Inertial Measurement Units (IMUs). IMUs are also used in satellites and robots [5] to help in navigation by reporting measures of orientation, velocity and acceleration. Calculation of displacements of limb joints is vital for posture recognition [13]. Monitoring the displacement of the entire body can be used for position estimation [1]. Multiple techniques have been used to gauge the displacement for applications that are not just pertaining to human motion.

The primary requisite for a sensor system is to have a small form factor to make it easily wearable. As in many portable electronic systems, the battery is the determining factor for the size of the system. Hence, by optimizing the power and improving the efficiency of the batteries with small form factors, the sensor system would become more portable and wearable. In this study, we try to achieve power optimization by turning off some of the sensors assuming their future measurements can be predicted by our model. For our model, we chose to turn off gyroscope while keeping accelerometers turned on. The rationale behind this choice is the higher power consumption of the gyroscopes. For the system used in our study, the typical power consumption of an accelerometer was 2.7 mW where as a gyroscope consumed 30 mW, which is an order of magnitude higher.

The system we used for prediction was based on Kalman filter. In our particular instance, the system was modeled based on walking, which meant that the state estimation would involve the calculation of displacement from the sensors. Calculation of displacement from the data provided by the accelerometer and gyroscope is often a complicated process. This is due to the presense of a bias offset in the accelerometer readings. The error due to a constant offset will polynomially increase with each integration to a level where the accuracy of the result will be lost. In [24], Zhongping et. al. have shown the basic scheme behind measuring the displacement along with the error analysis. In our model we implement a Kalman filter [6, 22] which would estimate

Permission to make digital or hard copies of all or part of this work for personal or classroom use is granted without fee provided that copies are not made or distributed for profit or commercial advantage and that copies bear this notice and the full citation on the first page. To copy otherwise, to republish, to post on servers or to redistribute to lists, requires prior specific permission and/or a fee.
Wireless Health '10, October 5-7, 2010, San Diego, USA
Copyright 2010 ACM 978-1-60558-989-3 ...$10.00.

the error during the integration and will correct it for every sample. This is accomplished by adding the bias as a state to be estimated and exploiting the rigid body nature of human limbs. Since the limbs are approximately rigid bodies, the position, linear velocity and angular velocity of sensors are constrained with respect to each other.

We experimented with different durations for which the sensor is switched off and plotted the reduction in accuracy. Results show an appreciable decrease in power consumption with a reasonable loss in accuracy. Further optimization is possible by calculating the ideal times for startup and shutdown of sensors and incorporating multiple sensor data for prediction. Future efforts will focus on such optimizations.

2. RELATED WORKS

A great amount of work has been done in the field of action recognition and position estimation using inertial measurement units. The sensors used in these IMUs are typically accelerometers and rate-gyroscopes. Initially, for applications such as action recognition and gait analysis, work had been done using only the accelerometer sensors. The authors in [2] use two miniature accelerometers to detect the gait cycle phases. This method was practical but did not prove to be very accurate, as single accelerations do not provide any input describing the change in direction of movement. To overcome this problem, rate-gyroscopes were coupled with the accelerometers to measure the angular velocity of the movements. Mayagoitia et al. [14] used this approach employing two sensors to obtain the gait kinematics.

Measuring the displacement or position can be a part of gait analysis [14]. The calculation of displacement or position is done for various applications. Authors in [3] used the IMUs for tremor sensing in Hand-held microsurgical instruments. The system was used to monitor the relative displacement of the surgical instrument from the origin. Similarly, [20] describe a method for measuring displacement based on inertial measuring system.

Kalman filtering is a statistical approach which reduces error due to random noise by combining knowledge of statistical errors and the system dynamics given by a state space model [6]. A variety of approaches exist for Kalman filtering. In [5], the authors used Extended Kalman Filter to generate error models for improving the accuracy of position and orientation estimation of a moving robotic vehicle. The authors of [11] and [15] use Adaptive Kalman Filtering for integrating the measurements from GPS with inertial navigation. The two main approaches are innovation-based adaptive estimation (IAE) and multiple-model-based adaptive estimation (MMAE)[15]. In our model, we use an innovation-based method for the state estimation and error correction.

Various methods for power optimization for Body Sensor Networks have been proposed in the past with many of them focusing on the number of active nodes used for monitoring. Ghasemzadeh et. al in [9] proposed a method to reduce the number of active nodes required for distinguishing the monitored activities. Similar methods have been proposed for Wireless Networks in [7], [18] and [21]. In all the above works, the focus has been to come up with a model to reduce the number of active sensors. Since different activities require different sets of sensor data, the above method requires change in the model for each activity.

This paper focuses on the design of a suitable model for prediction of sensor data and its validation. The method illustrated in this paper is efficient when a single node consists of multiple sensors, some of which have higher power consumption compared to others. The power-heavy sensors can be turned off periodically while their data is predicted using our model, based on previous measurements and the readings from other sensors. It is possible to generalize this method to different type of sensors as long as the combination of sensor data defines a state.

3. SYSTEM DESIGN

In this section we will describe our model and the signal processing.

3.1 Sensing Platform

Our experimental setup comprises of TelosB motes, shown in Figure 1, with custom-designed sensor board mounted on the mote. Each sensor board consists of one tri-axial accelerometer and one bi-axial gyroscope. The digital accelerometers used can record an acceleration upto 2g, at a sensitivity of $1024LSb/g$. The analog rate-gyros used in these boards are SparkFun IDG-300 which has a sensitivity of $2mV/\deg/s$. Each mote collects data and transfers it to the base station wirelessly. The frequency of sampling used is 50Hz. The base station is a mote without the sensor board which is connected to the Personal Computer via a USB cable. The base station forwards the packets received from other motes to the PC. We have a MATLAB tool on the PC side for collecting and ordering the data.

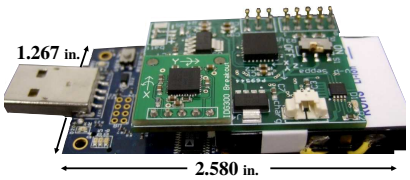

Figure 1: TelosB Mote

3.2 Signal Processing

The raw data obtained from the sensor has to be initially converted and calibrated. The output of the accelerometer is in g-force which is changed to m/s^2 and the gyroscope readings converted to $\deg/s$. Removing the gravity component from the accelerometer data is done through the an orientation estimate acquired by integrating the rate-gyros. The angle of inclination θ is obtained from the gyroscope[23] and the magnitude of acceleration due to gravity is split along the axes of each accelerometer and removed.

The estimate of position from the acceleration is mathematically a double integration of the acceleration. A cumulative trapezoidal integration is generally done on the acceleration vector to obtain the velocity estimate of every sample. The same integration is performed again to get the position vector. The method elaborated above is a typical way of calculating the velocity and position components from the accelerometer sensor. The limitation here is that the integration does not account for the bias offset which would cause a drift error that increases polynomially with time. The Kalman filter defined in our model accounts for this bias error and does not include it in the integration.

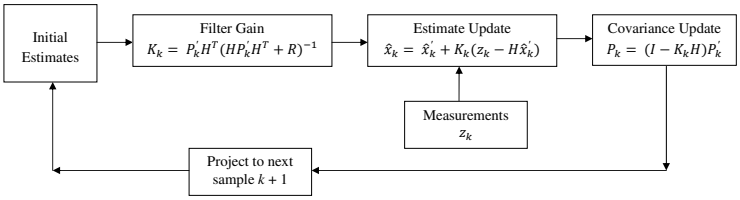

Figure 2: Flow of Kalman Filter Operation

Table 1: Definition of Variables

Variables	Definitions
K_k	Kalman Gain
P_k	Error Covariance Matrix
R	Covariance of Measurement Error
Q	Covariance of Process Noise

3.3 Kalman Filter

In this section, a general Kalman filter is illustrated. The basic theory behind Kalman filter is described in detail in many sources [6, 22]. The operational flow can be seen in Figure 2. The definition of variables are provided in Table 1. Consider the linear, discrete-time system;

$$x_{k+1} = Ax_k + \omega_k \quad (1)$$

$$y_k = Hx_k + \nu_k \quad (2)$$

where $k \in \{1, 2, ...\}$ is a the discrete time index, $x_k \in \Re^n$ is the system state at time k, $y_k \in \Re^m$ is the measurement vector at time k, $A \in \Re^{n \times n}$ is the state transition matrix that describes the evolution of x_k over time, $H_k \in \Re^{m \times n}$ is a matrix mapping the state to the measurement vector, and $\omega_k \in \Re^n$ and $\nu_k \in \Re^n$ are white, zero-mean, Gaussian, noise process with covariance matrices $Q \in \Re^{n \times n}$ and $R \in \Re^{m \times m}$, respectively.

The well known Kalman Filter equations [6] provide an optimal estimate in the sense that it is the minimum mean square error estimate for linear estimators. The one-step KF equations are given as;

$$\hat{x}_{k+1} = A\hat{x}_k + K_k(y_k - H\hat{x_k}) \quad (3)$$

$$K_k = AP_k H^T (R + HP_k H^T)^{-1} \quad (4)$$

$$P_k = A(P_k^{-1} + H^T R^{-1} H)^{-1} A^T + Q \quad (5)$$

where K_k is the Kalman gain and P_k is the covariance of the estimate error $e_k = \hat{x}_k - x_k$. The overall model of the Kalman filter is shown in Figure 2.

The main objective of a Kalman filter is to use the measurments data y_k to find the minimum mean square estimate of the state matrix x_k. The estimate of $\hat{x}_k$ is calculated by the knowledge of the system in A_k and $\hat{x}_{k-1}$. The *innovation* of the model is necessarily the error which is the difference between the real value and the estimated value by the filter. It can be denoted by z_k which is given by;

$$z_k = y_k - H\hat{x}_k \quad (6)$$

There is always a difference between the actual measurement and the estimated measurement. This innovation, along with the filter gain K_k is used to correct the estimate of the component in the next time step. This process is done recursively for all time steps.

4. IMPLEMENTATION

In the following subsections we describe the initial setup and its methodology.

4.1 Experimental Setup

Figure 3: Mote Placement

For our experiment, two sensors were placed on the right leg of the subject. Mote one was placed on the thigh and mote two was placed just below the knee. This can be seen in Figures 3 and 4. As discussed previously, each mote has two sensors incorporated in it, one three axis accelerometer and one two axis gyroscope. The sensors were oriented initially such that the $x - axis$ of the accelerometer pointed distally and the $z - axis$ pointed laterally. The $y - axis$ of the gyroscope is in a direction such that it can measure the angular swing of the knee while walking. All the motes were placed in an almost collinear manner so that there would be only small offsets among them. Each mote runs an individual Kalman filter.

4.2 Initial Measurements

Before beginning the experiment, certain assumptions were made on the basis of the position and orientation of the motes. Figure 4 shows the direction of axis of each sensor and also the angles of inclination with respect to the gravity vector. The initial values of θ_1 and θ_2 were taken as zero considering the subject to be standing still. The angular velocities ω_1 and ω_2 were also zero due to the same reason. The sensor readings are acquired at a sampling rate of $50Hz$.

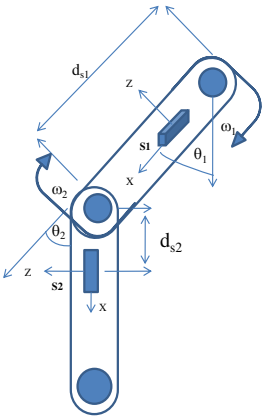

Figure 4: Modeling of the leg as linked rigid bodies

4.3 Implementation Details

The two Kalman filters are set up as discussed in Section 3.3. The state and measurement matrices can be seen in the appendix sections 8.1 and 8.2. The process noise Q (section 3.3, equation 5) is modeled as zero-mean gaussian white noise with the covariance given by a *random walk* process. The process noise matrices are shown in the appendix section 8.3. The covariance matrix of the measurement noise R (section 3.3, equations 4 and 5) is a diagonal matrix whose values were obtained by calculating the variance of the readings from the sensor when placed still for several seconds.

During walking, the accelerometer and gyroscope sensors measure the acceleration and angular velocity components. The frequency of sampling was $50Hz$. This helps in reducing the error in estimating the change in angles θ_1 and θ_2 shown in Figure 4. Gyroscope 2 is powered on alternatively after a particular sample of time. This results in increasing the life time of the sensor as it is not being operated for the entire experiment. The results of our experiments are shown in the next section. The equation below is used for calculating the linear velocity from the angular velocity obtained from the gyroscopes.

$$\begin{bmatrix} \dot{x}_{s1g1} \\ \dot{z}_{s1g1} \\ \dot{x}_{s2g2} \\ \dot{z}_{s2g2} \end{bmatrix} = \begin{bmatrix} -d_{s1}sin\theta_1 & 0 \\ d_{s1}cos\theta_1 & 0 \\ -d_{s1}sin\theta_1 & -d_{s2}sin\theta_2 \\ d_{s1}cos\theta_1 & d_{s2}cos\theta_2 \end{bmatrix} \begin{bmatrix} \omega_{1g1} \\ \omega_{2g2} \end{bmatrix}$$

In the above equation, ω_{1g1} and ω_{2g2} are the angular velocity measurements obtained from gyroscopes 1 and 2. The angles θ_1 and θ_2, and the displacement of the two sensors from joints d_{s1} and d_{s2}, are marked in figure 4. The linear velocity estimates $\dot{x}_{s1g1}$, $\dot{x}_{s2g2}$, $\dot{z}_{s1g1}$ and $\dot{z}_{s2g2}$ are then fed into the measurement equations defined in section 8.2 provided for the thigh and the shin sensors.

5. RESULTS

Figure 5 shows the output from the gyroscope on the first mote which was placed on the thigh. The Kalman filter provides a smoother version of the actual data by reducing the error in measured signal. Similar waveforms can be observed for the gyroscope on the second mote.

The power optimization was performed for the second gyroscope, which was placed below the knee. Figure 6 shows the Kalman estimates for the second gyroscope with and without the power savings, and the error introduced by the power optimization.

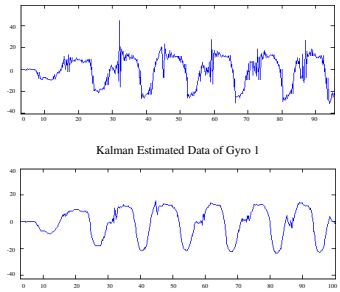

Figure 5: Output of Gyroscope 1

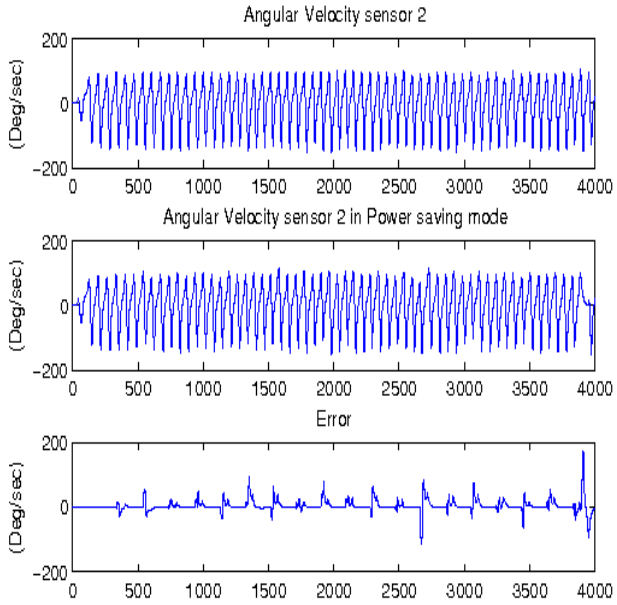

Figure 6: Gyroscope Output in Power Saver Mode

In the power saving mode, the gyroscope 2 is powered off periodically while the data is replicated from the previous cycle for which it was on. The Kalman estimate of this modified data is then compared with the Kalman estimate generated for the sensor data obtained without powering off. The gyroscope requires time of $200ms$ to power up and stabilize before collecting data. This means that the total power savings is slightly less than the time for which the gyroscope is inactive (i.e. not taking measurements). Table 2 shows this mapping between the measurement period and the power savings. In the table, duty cycle is the ratio of active time with respect to total duration of experiment. The active time does not include initial setup time for the gyroscope. The energy savings obtained by this method is plotted against the error in figure 7. The error is represented by the percentage of RMS value of the error signal with respect to the RMS of Kalman estimate of angular velocity.

Table 2: Power Performance

Configuration	Duty Cycle (%)	Energy Savings (%)	RMS Error
1	90	8.57	0.1259
2	80	17.14	0.1871
3	70	28.57	0.2195
4	60	37.14	0.2266
5	50	42.86	0.2509
6	40	57.14	0.2667
7	30	68.57	0.2570
8	20	77.14	0.2804
9	10	88.57	0.3022

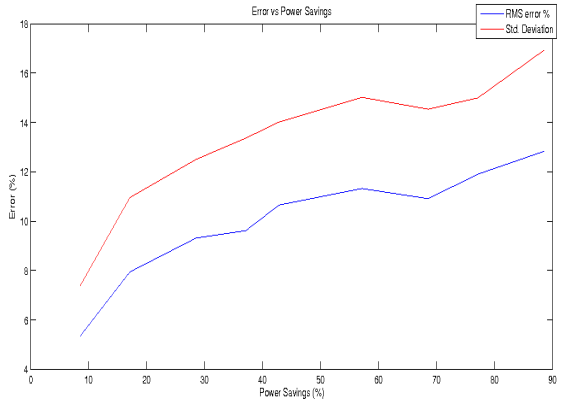

Figure 7: Error vs Power savings

The standard deviation of the error measurements is also plotted in figure 7. The error increases with decrease in the active time as expected. Depending on the fidelity required for the sensor measurements and the duration over which the measurements are to be taken, we can choose an appropriate turn-off period without significant loss of accuracy.

6. CONCLUSION

In our work, we investigated power optimization for Body Sensor Networks by turning off sensors. We applied Kalman filter to model the output of a sensor based on previous measurements and current readings from other sensors. Based on the pilot experiments we have conducted, the proposed model shows significant power savings of above 60% with acceptable estimation of the reproduced signal. Since the tolerable limits for error are dependent on the application, we have plotted the variation in error with respect to the accuracy. In future, we will investigate power reduction techniques when the sensors can remain inactive for a longer period of time, and an error function generated by the Kalman filter will determine when the sensors should be activated. Furthermore, we will formally define and attempt to minimize an objective function which incorporates the power consumption of every sensor.

7. REFERENCES

[1] J. Albowicz, A. Chen, and L. Zhang. Recursive position estimation in sensor networks. In *IEEE Int. Conf. on Network Protocols*, pages 35–41. Citeseer, 2001.

[2] K. Aminian, K. Rezakhanlou, E. De Andres, C. Fritsch, P. Leyvraz, and P. Robert. Temporal feature estimation during walking using miniature accelerometers: an analysis of gait improvement after hip arthroplasty. *Medical and Biological Engineering and Computing*, 37(6):686–691, 1999.

[3] W. Ang, P. Khosla, and C. Riviere. Design of all-accelerometer inertial measurement unit for tremor sensing in hand-held microsurgical instrument. In *IEEE International Conference on Robotics and Automation*, volume 2, pages 1781–1786. Citeseer, 2003.

[4] J. Barnes and R. Jafari. Locomotion monitoring using body sensor networks. In *Proceedings of the 1st international conference on PErvasive Technologies Related to Assistive Environments*, page 47. ACM, 2008.

[5] B. Barshan and H. Durrant-Whyte. Inertial navigation systems for mobile robots. *Robotics and Automation, IEEE Transactions on*, 11(3):328 –342, jun 1995.

[6] R. Brown. *Introduction to random signal analysis and Kalman filtering*. Wiley New York, 1983.

[7] M. Cardei, D. MacCallum, M. X. Cheng, M. Min, X. Jia, D. Li, and D.-Z. Du. Wireless sensor networks with energy efficient organization. *JOURNAL OF INTERCONNECTION NETWORKS*, 3(3/4):213–230, 2002.

[8] J. Chen, K. Kwong, D. Chang, J. Luk, and R. Bajcsy. Wearable sensors for reliable fall detection. In *Engineering in Medicine and Biology Society, 2005. IEEE-EMBS 2005. 27th Annual International Conference of the*, pages 3551–3554, 2005.

[9] H. Ghasemzadeh, E. Guenterberg, K. Gilani, and R. Jafari. Action coverage formulation for power optimization in body sensor networks. In *ASP-DAC '08: Proceedings of the 2008 Asia and South Pacific Design Automation Conference*, pages 446–451, Los Alamitos, CA, USA, 2008. IEEE Computer Society Press.

[10] H. Ghasemzadeh, V. Loseu, E. Guenterberg, and R. Jafari. Sport training using body sensor networks: a statistical approach to measure wrist rotation for golf swing. In *Proceedings of the Fourth International Conference on Body Area Networks*, pages 1–8. ICST (Institute for Computer Sciences, Social-Informatics and Telecommunications Engineering), 2009.

[11] C. Hide, T. Moore, and M. Smith. Adaptive kalman filtering algorithms for integrating gps and low cost

ins. In *Position Location and Navigation Symposium, 2004. PLANS 2004*, pages 227 – 233, 26-29 2004.

[12] E. Jovanov, A. Milenkovic, C. Otto, and P. de Groen. A wireless body area network of intelligent motion sensors for computer assisted physical rehabilitation. *Journal of NeuroEngineering and Rehabilitation*, 2(1):6, 2005.

[13] F. Lorussi, W. Rocchia, E. Scilingo, A. Tognetti, and D. De Rossi. Wearable, redundant fabric-based sensor arrays for reconstruction of body segment posture. *IEEE Sensors Journal*, 4(6):807–818, 2004.

[14] R. Mayagoitia, A. Nene, and P. Veltink. Accelerometer and rate gyroscope measurement of kinematics: an inexpensive alternative to optical motion analysis systems. *Journal of Biomechanics*, 35(4):537–542, 2002.

[15] A. Mohamed and K. Schwarz. Adaptive Kalman filtering for INS/GPS. *Journal of Geodesy*, 73(4):193–203, 1999.

[16] J. D. O'Sullivan, C. M. Said, L. C. Dillon, M. Hoffman, and A. J. Hughes. Gait analysis in patients with Parkinson's disease and motor fluctuations: Influence of levodopa and comparison with other measures of motor function. *Movement Disorders*, 13(6):900–906, 1998.

[17] C. Otto, A. Milenkovic, C. Sanders, and E. Jovanov. System architecture of a wireless body area sensor network for ubiquitous health monitoring. *Journal of Mobile Multimedia*, 1(4):307–326, 2006.

[18] S. Slijepcevic and M. Potkonjak. Power efficient organization of wireless sensor networks. In *Communications, 2001. ICC 2001. IEEE International Conference on*, volume 2, pages 472 –476 vol.2, 2001.

[19] O. Sofuwa, A. Nieuwboer, K. Desloovere, A.-M. Willems, F. Chavret, and I. Jonkers. Quantitative Gait Analysis in Parkinson's Disease: Comparison With a Healthy Control Group. *Archives of Physical Medicine and Rehabilitation*, 86(5):1007 – 1013, 2005.

[20] I. Tien, S. D. Glaser, R. Bajcsy, D. S. Goodin, and M. J. Aminoff. Results of using a wireless inertial measuring system to quantify gait motions in control subjects. *Information Technology in Biomedicine, IEEE Transactions on*, 14(4):904 –915, july 2010.

[21] X. Wang, J. jie Ma, S. Wang, and D. wei Bi. Prediction-based dynamic energy management in wireless sensor networks. *Sensors 2007*, 7:251–266, 2007.

[22] G. Welch and G. Bishop. An introduction to the Kalman filter. *University of North Carolina at Chapel Hill, Chapel Hill, NC*, 1995.

[23] R. Williamson and B. Andrews. Detecting absolute human knee angle and angular velocity using accelerometers and rate gyroscopes. *Medical and Biological Engineering and Computing*, 39(3):294–302, 2001.

[24] R. Zhongping and X. Songmei. The Principle of Measuring the Displacement with Accelerometer and the Error Analysis [J]. *Journal of Huazhong University of Science and Technology*, 5, 2000.

8. APPENDIX

8.1 State Transition Matrices

$\hat{x}_{k+1} = A_k \hat{x}_k$

Thigh Sensor

$$\begin{bmatrix} x_{s1} \\ \dot{x}_{s1} \\ \ddot{x}_{s1} \\ z_{s1} \\ \dot{z}_{s1} \\ \ddot{z}_{s1} \\ v \\ \theta_1 \\ \omega_1 \end{bmatrix} = \begin{bmatrix} 1 & \Delta T & 0 & 0 & 0 & 0 & 0 & 0 & 0 \\ 0 & 1 & \Delta T & 0 & 0 & 0 & 0 & 0 & 0 \\ 0 & 0 & 1 & 0 & 0 & 0 & 0 & 0 & 0 \\ 0 & 0 & 1 & \Delta T & 0 & 0 & 1 & 0 & 0 \\ 0 & 0 & 0 & 0 & 1 & \Delta T & 0 & 0 & 0 \\ 0 & 0 & 0 & 0 & 0 & 1 & 0 & 0 & 0 \\ 0 & 0 & 0 & 0 & 0 & 0 & 1 & 0 & 0 \\ 0 & 0 & 0 & 0 & 0 & 0 & 0 & 1 & \Delta T \\ 0 & 0 & 0 & 0 & 0 & 0 & 0 & 0 & 1 \end{bmatrix} \begin{bmatrix} x_{s1} \\ \dot{x}_{s1} \\ \ddot{x}_{s1} \\ z_{s1} \\ \dot{z}_{s1} \\ \ddot{z}_{s1} \\ v \\ \theta_1 \\ \omega_1 \end{bmatrix}$$

Shin Sensor

$$\begin{bmatrix} x_{s2} \\ \dot{x}_{s2} \\ \ddot{x}_{s2} \\ z_{s2} \\ \dot{z}_{s2} \\ \ddot{z}_{s2} \\ v \\ \theta_1 \\ \omega_1 \\ \theta_2 \\ \omega_2 \end{bmatrix} = \begin{bmatrix} 1 & \Delta T & \Delta T^2 & 0 & 0 & 0 & 0 & 0 & 0 & 0 & 0 \\ 0 & 1 & \Delta T & 0 & 0 & 0 & 0 & 0 & 0 & 0 & 0 \\ 0 & 0 & 1 & 0 & 0 & 0 & 0 & 0 & 0 & 0 & 0 \\ 0 & 0 & 0 & 1 & \Delta T & \Delta T^2 & 0 & 0 & 0 & 0 & 0 \\ 0 & 0 & 0 & 0 & 1 & \Delta T & 0 & 0 & 0 & 0 & 0 \\ 0 & 0 & 0 & 0 & 0 & 1 & 0 & 0 & 0 & 0 & 0 \\ 0 & 0 & 0 & 0 & 0 & 0 & 1 & 0 & 0 & 0 & 0 \\ 0 & 0 & 0 & 0 & 0 & 0 & 0 & 1 & 0 & \Delta T & 0 \\ 0 & 0 & 0 & 0 & 0 & 0 & 0 & 0 & 1 & 0 & 0 \\ 0 & 0 & 0 & 0 & 0 & 0 & 0 & 0 & 0 & 1 & \Delta T \\ 0 & 0 & 0 & 0 & 0 & 0 & 0 & 0 & 0 & 0 & 1 \end{bmatrix} \begin{bmatrix} x_{s2} \\ \dot{x}_{s2} \\ \ddot{x}_{s2} \\ z_{s2} \\ \dot{z}_{s2} \\ \ddot{z}_{s2} \\ v \\ \theta_1 \\ \omega_1 \\ \theta_2 \\ \omega_2 \end{bmatrix}$$

Variables	Definition
x_{s1}, x_{s2}	Estimate of position from x-azis of sensors 1, 2
$\dot{x}_{s1}, \dot{x}_{s2}$	Estimate of velocity from x-axis sensors 1, 2
$\ddot{x}_{s1}, \ddot{x}_{s2}$	Estimate of acceleration from x-axis sensors 1, 2
z_{s1}, z_{s2}	Estimate of position from z-azis of sensors 1, 2
$\dot{z}_{s1}, \dot{z}_{s2}$	Estimate of velocity from z-axis sensors 1, 2
$\ddot{z}_{s1}, \ddot{z}_{s2}$	Estimate of acceleration from z-axis sensors 1, 2
ω_1, ω_2	Estimate of angular velocity from sensors 1, 2

Table 3: Definition of Variables

8.2 Measurement Equations

$y_k = H \hat{x}_k$

Thigh Sensor

$$\begin{bmatrix} \dot{x}_{s1g1} \\ \dot{z}_{s1g1} \\ \ddot{x}_{s1a1} \\ \ddot{z}_{s1a1} \\ \omega_{1g1} \end{bmatrix} = \begin{bmatrix} 0 & 1 & 0 & 0 & 0 & 0 & 0 & -1 & 0 \\ 0 & 0 & 0 & 0 & 1 & 0 & 0 & -1 & 0 \\ 0 & 0 & 1 & 0 & 0 & 0 & 0 & 0 & 0 \\ 0 & 0 & 0 & 0 & 0 & 1 & 0 & 0 & 0 \\ 0 & 0 & 0 & 0 & 0 & 0 & 0 & 0 & 1 \end{bmatrix} \begin{bmatrix} x_{s1} \\ \dot{x}_{s1} \\ \ddot{x}_{s1} \\ z_{s1} \\ \dot{z}_{s1} \\ \ddot{z}_{s1} \\ v \\ \theta_1 \\ \omega_1 \end{bmatrix}$$

Shin Sensor

$$\begin{bmatrix} \ddot{x}_{s2a2} \\ \ddot{z}_{s2a2} \\ \dot{x}_{s2g2} \\ \dot{z}_{s2g2} \\ \omega_{2g2} \end{bmatrix} = \begin{bmatrix} 0 & 0 & 1 & 0 & 0 & 0 & 0 & 0 & 0 & 0 & 0 \\ 0 & 0 & 0 & 0 & 0 & 1 & 0 & 0 & 0 & 0 & 0 \\ 0 & 0 & 0 & 0 & 0 & 0 & 0 & 0 & 0 & a1 & b1 \\ 0 & 0 & 0 & 0 & 0 & 0 & 0 & 0 & 0 & a2 & b2 \\ 0 & 0 & 0 & 0 & 0 & 0 & 0 & 0 & 0 & 0 & 1 \end{bmatrix} \begin{bmatrix} x_{s2} \\ \dot{x}_{s2} \\ \ddot{x}_{s2} \\ z_{s2} \\ \dot{z}_{s2} \\ \ddot{z}_{s2} \\ v \\ \theta_1 \\ \theta_2 \\ \omega_1 \\ \omega_2 \end{bmatrix}$$

Variables	Definition
$\ddot{x}_{s1a1}, \ddot{x}_{s2a2}$	Measurement of acceleration from x-axis of sensors 1, 2
$\ddot{z}_{s1a1}, \ddot{z}_{s2a2}$	Measurement of acceleration from z-axis of sensors 1, 2
$\dot{x}_{s1g1}, \dot{x}_{s2g2}$	Measurement of velocity from x-axis gyroscope of sensors 1, 2
$\dot{z}_{s1g1}, \dot{z}_{s2g2}$	Measurement of velocity from z-axis gyroscope of sensors 1, 2
$\omega_{1g1}, \omega_{2g2}$	Measurement of angular velocity from sensors 1, 2

Table 4: Definition of Variables

8.3 Process Noise Matrices

$Q_{Thigh}=$

$$\begin{bmatrix} \frac{\sigma*\Delta T^9}{9} & \frac{\sigma*\Delta T^4}{4} & \frac{\sigma*\Delta T^5}{5} & 0 & 0 & 0 & 0 & 0 & 0 \\ \frac{\sigma*\Delta T^4}{4} & \frac{\sigma*\Delta T^3}{3} & \frac{\sigma*\Delta T^2}{2} & 0 & 0 & 0 & 0 & 0 & 0 \\ \frac{\sigma*\Delta T^5}{5} & \frac{\sigma*\Delta T^2}{2} & \sigma*\Delta T & 0 & 0 & 0 & 0 & 0 & 0 \\ 0 & 0 & 0 & \frac{\sigma*\Delta T^9}{9} & \frac{\sigma*\Delta T^4}{4} & \frac{\sigma*\Delta T^5}{5} & 0 & 0 & 0 \\ 0 & 0 & 0 & \frac{\sigma*\Delta T^4}{4} & \frac{\sigma*\Delta T^3}{3} & \frac{\sigma*\Delta T^2}{2} & 0 & 0 & 0 \\ 0 & 0 & 0 & \frac{\sigma*\Delta T^5}{5} & \frac{\sigma*\Delta T^2}{2} & \sigma*\Delta T & 0 & 0 & 0 \\ 0 & 0 & 0 & 0 & 0 & 0 & \frac{\sigma*\Delta T^9}{9} & \frac{\sigma*\Delta T^4}{4} & \frac{\sigma*\Delta T^5}{5} \\ 0 & 0 & 0 & 0 & 0 & 0 & \frac{\sigma*\Delta T^4}{4} & \frac{\sigma*\Delta T^3}{3} & \frac{\sigma*\Delta T^2}{2} \\ 0 & 0 & 0 & 0 & 0 & 0 & \frac{\sigma*\Delta T^5}{5} & \frac{\sigma*\Delta T^2}{2} & \sigma*\Delta T \end{bmatrix}$$

$Q_{Shin}=$

$$\begin{bmatrix} \frac{\sigma*\Delta T^9}{9} & \frac{\sigma*\Delta T^4}{4} & \frac{\sigma*\Delta T^5}{5} & 0 & 0 & 0 & 0 & 0 & 0 & 0 & 0 \\ \frac{\sigma*\Delta T^4}{4} & \frac{\sigma*\Delta T^3}{3} & \frac{\sigma*\Delta T^2}{2} & 0 & 0 & 0 & 0 & 0 & 0 & 0 & 0 \\ \frac{\sigma*\Delta T^5}{5} & \frac{\sigma*\Delta T^2}{2} & \sigma*\Delta T & 0 & 0 & 0 & 0 & 0 & 0 & 0 & 0 \\ 0 & 0 & 0 & \frac{\sigma*\Delta T^9}{9} & \frac{\sigma*\Delta T^4}{4} & \frac{\sigma*\Delta T^5}{5} & 0 & 0 & 0 & 0 & 0 \\ 0 & 0 & 0 & \frac{\sigma*\Delta T^4}{4} & \frac{\sigma*\Delta T^3}{3} & \frac{\sigma*\Delta T^2}{2} & 0 & 0 & 0 & 0 & 0 \\ 0 & 0 & 0 & \frac{\sigma*\Delta T^5}{5} & \frac{\sigma*\Delta T^2}{2} & \sigma*\Delta T & 0 & 0 & 0 & 0 & 0 \\ 0 & 0 & 0 & 0 & 0 & 0 & \sigma*\Delta T & 0 & 0 & 0 & 0 \\ 0 & 0 & 0 & 0 & 0 & 0 & 0 & \frac{\sigma*\Delta T^3}{3} & \frac{\sigma*\Delta T^2}{2} & 0 & 0 \\ 0 & 0 & 0 & 0 & 0 & 0 & 0 & \frac{\sigma*\Delta T^2}{2} & \sigma*\Delta T & 0 & 0 \\ 0 & 0 & 0 & 0 & 0 & 0 & 0 & 0 & 0 & \frac{\sigma*\Delta T^3}{3} & \frac{\sigma*\Delta T^2}{2} \\ 0 & 0 & 0 & 0 & 0 & 0 & 0 & 0 & 0 & \frac{\sigma*\Delta T^2}{2} & \sigma*\Delta T \end{bmatrix}$$